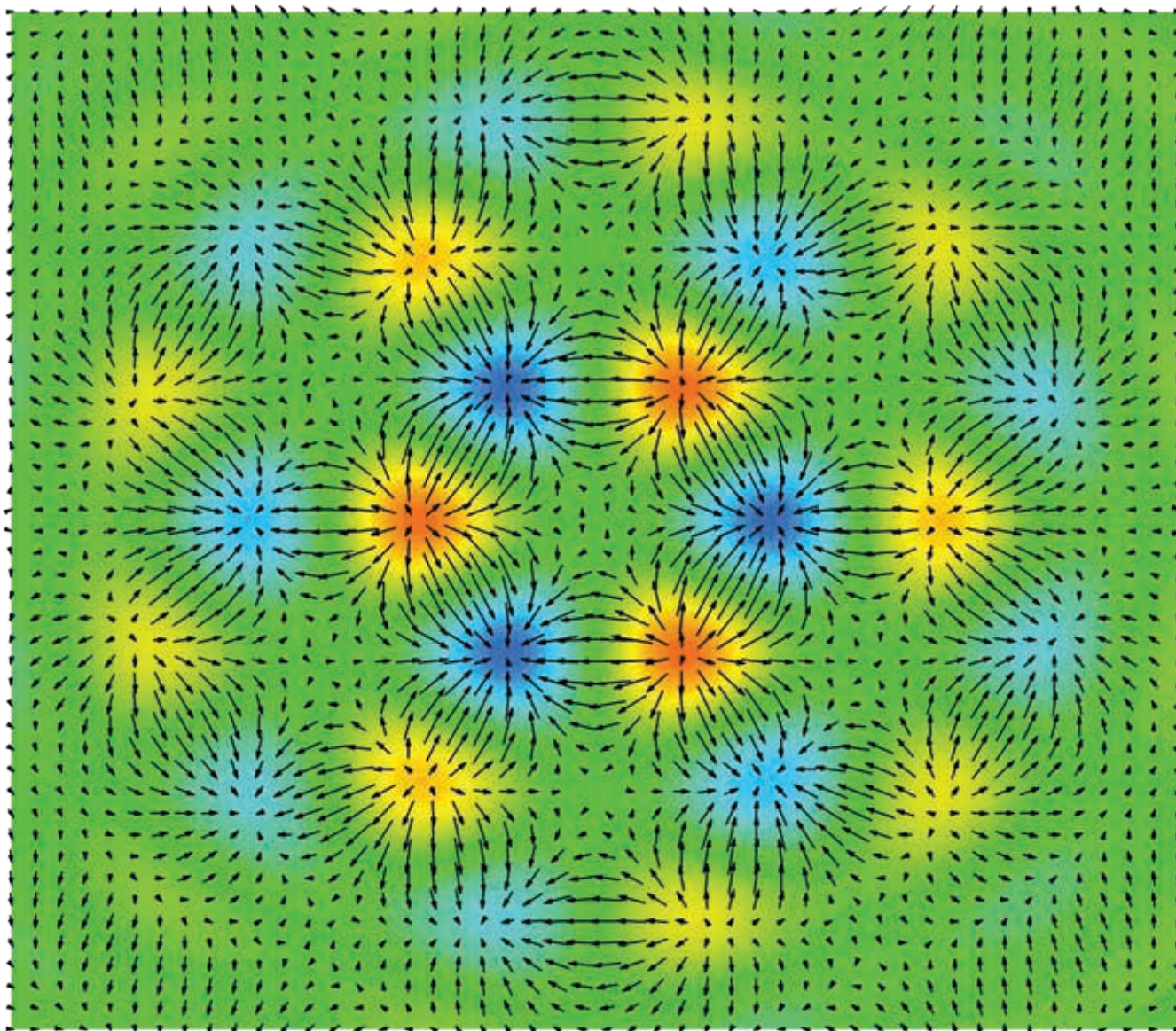


APPN

ASIA PACIFIC PHYSICS NEWSLETTER

May 2012 • Volume 1 • Number 1

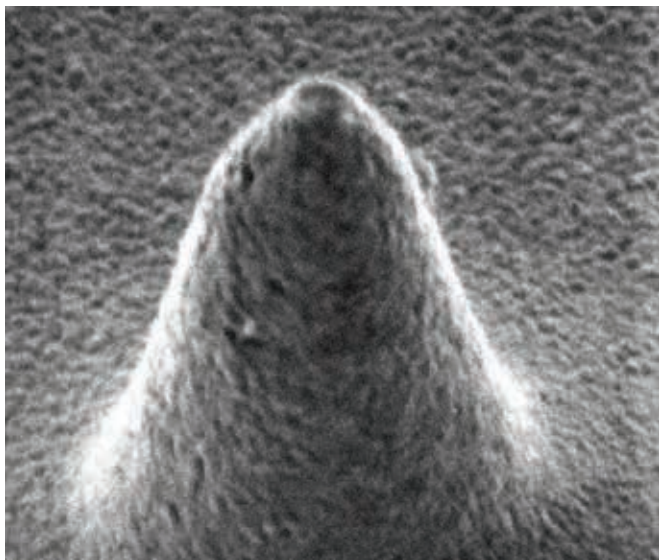
A publication of the SEATPA and IAS@NTU Singapore



Fermi's β -decay Theory

Chandrasekhar and the History of Astronomy

Quantum Numbers, Chern Classes, and a Bodhisattva



(b) Scanning ion microscope image of a double tapered near-field optical fiber probe.

with increase in magnetic field in accordance with a theoretical model by Chklovskii, Shklovskii and Glazman [1]. Mapping of quantum Hall edge states by using a near-field scanning optical microscope has revealed how compressible-incompressible strips develop with magnetic field at the presence of disorders. Furthermore, mapping of quantum Hall edge states enables us to clarify how the change in the coupling between bulk and edge affects the motion of the optically created electrons in an inhomogeneous electrostatic potential in the vicinity of the edge of a quantum Hall liquid.

Our success in direct mapping of the quantum Hall edge states is a major step forward in nano-transport and nano-optics research and will contribute to image such as a fractional quantum-Hall phase and a quantum anomalous Hall phase.

[1] D.B. Chklovskii, B.I. Shklovskii, and L.I. Glazman, *Phys. Rev. B* **46**, 4026 (1992).

H. Ito, K. Furuya, Y. Shibata, S. Kashiwaya, M. Yamaguchi, T. Akazaki, H. Tamura, Y. Ootuka and S. Nomura, “Near-Field Optical Mapping of Quantum Hall Edge States”, *Phys. Rev. Lett.* **107**, 256803 (2011)

Electro-Rheological Fluids

Maxwell Stress in Fluid Mixtures

A rapid and reversible change of fluid viscosity by electric field is referred to as the electro-rheological (ER) effect, which is of great technological importance in industry. In the present paper, we derive a new formula for the Maxwell stress, a fundamental physical quantity controlling the ER

effect. Identifying the Maxwell stress contribution as an excess anisotropic interfacial tension, the formula should be useful to investigate the physics of various class of electro-(magneto-)rheological fluids.

T. Sakaue and T. Ohta,

“Maxwell Stress in Fluid Mixtures”, *Phys. Rev. Lett.* **108**, 078301 (2012)

Percolation Transition

Suppression Effect on Explosive Percolation

When a group of people unknown to each other meet and familiarize among themselves, over time they form a community on a macroscopic scale. This phenomenon can be understood in the context of percolation transition (PT) of networks. It is well known that the PT takes place continuously in the classical random graph model introduced by Erdos and Renyi (ER), in which a system composed of a fixed number of vertices N evolves as edges are added. At each evolution step, an edge is added between two vertices, which are selected randomly among unconnected pairs of vertices. This ER model has been modified by Achlioptas et al., who designed it to suppress the formation of the giant cluster: Two edge candidates are randomly selected, but only one of them is actually added to the system, which is the one minimizing the product or the sum of the sizes of the clusters that are connected by each potential edge. In these models, the giant cluster size increases drastically at the critical point and thus the percolation transition is called explosive percolation. This explosive PT model has triggered intensive researches on discontinuous PTs in nonequilibrium systems. Many models have followed these models and display similar transition patterns. Although this explosive PT was regarded as discontinuous in the original paper, it has been argued that the transition is continuous in the thermodynamic limit. Thus, the issue whether the explosive PT is indeed discontinuous or continuous remains controversial. In our work, we investigate the dynamic rules of several explosive percolation models microscopically, and find amazingly that those rules do not follow the so-called suppression principle. The Achlioptas process essentially identifies the dynamics that prevent the creation of a given target pattern by choosing one edge from a given number of randomly selected potential edges. Since the target pattern in the modified ER model is a giant cluster, an edge to be added actually to the system should be selected such that the growth of clusters can be systematically suppressed. The

current models people discussed do not fulfill such principle. Thus, it is rather natural that the PTs of those models are continuous. However, some other variants of the Achlioptas model satisfying the suppression principle exhibit the pattern of discontinuous PTs within the range of our numerical simulations. Thus, in this paper, we argue that satisfying the suppression principle is essential for discontinuous PTs.

Y. S. Cho and B. Kahng,

“Suppression Effect on Explosive Percolation”, *Phys. Rev. Lett.* **107**, 275703 (2011).

Topological Insulator

Chiral Orbital-Angular Momentum in the Surface States of Bi_2Se_3

Surface states of topological insulators (TIs) possess exotic properties. One of them is locking of the electron spin to the momentum, resulting in a chiral spin structure in the surface states. This spin texture suppresses backscattering and thus promotes the possibility for TIs to be used for spin conserving media in spintronics. While chiral spin texture is well studied, orbital-angular momentum (OAM) in TIs has drawn very little attention. However, strong spin-orbit interaction in high-Z materials tends to restore a local OAM, and such local OAM must also have chiral structure by symmetry. Existence of chiral OAM in the surface states is important because it is the OAM that governs the energetics of the surface states[1]. In addition, OAM is also important for optical properties of TIs since the OAM directly couples to the electric field of light.

In their paper, Park et al. studied the surface states of Bi_2Se_3 by means of angle-resolved photoelectron spectroscopy (ARPES) with circularly polarized light and first-principles calculation. They found that there is strong circular dichroism (CD) in ARPES data from Bi_2Se_3 surface states. It is shown that such CD signal is approximately proportional to OAM, suggesting that the surface states may possess substantial chiral OAM. First-principles calculation result shows that the chiral OAM has a sizable magnitude and thus proves the conclusion extracted from the experimental results.

Existence of chiral OAM, oppositely aligned to the electron spin as summarized in the figure, implies not only the spin but also OAM can play an important role in the surface state properties. An important aspect is on the coupling between light and electronic states because it is the orbital part of the wave function that directly couples to the electric field of light. As an example, they discuss possibility

of light-induced spin (and also OAM) polarized current in the surface states. This implies that a spin polarized current can be controlled by the polarization of the light.

[1] S. R. Park, C. H. Kim, J. Yu, J. H. Han, and C. Kim, *Phys. Rev. Lett.* **107**, 156803 (2011).

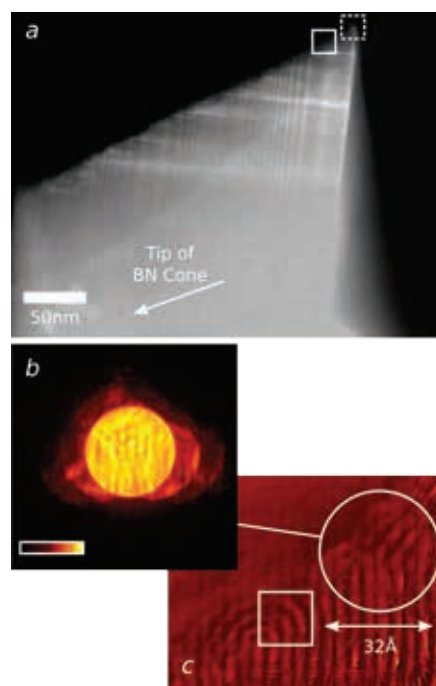
S. R. Park, J. Han, C. Kim, Y. Y. Koh, C. Kim, H. Lee, H. J. Choi, J. H. Han, K. D. Lee, N. J. Hur, M. Arita, K. Shimada, H. Namatame and M. Taniguchi,

“Chiral Orbital-Angular Momentum in the Surface States of Bi_2Se_3 ”, *Phys. Rev. Lett.* **108**, 046805 (2012)

Electron Microscope

Atom-Scale Ptychographic Electron Diffractive Imaging of Boron Nitride Cones

Microscopy plays a key role in structure determination at length scales ranging from microns, in a typical optical microscope, to angstroms, in modern day electron microscopes. The ability of a microscope to obtain beautiful, high resolution images is often limited by the focusing optics in the imaging system. Coherent diffractive imaging, or CDI, is a microscopy technique which circumvents the requirement for focusing optics, instead collecting the raw diffraction signal after it has interacted with the specimen, and using



(a) Large annular dark-field image of a Boron-Nitride cone used to demonstrate the technique, showing the region of interest imaged in (c) as a small solid white box. A sample of one of the fifteen recorded diffraction patterns used to construct the CDI image is shown in (b), with the final image shown in (c).